A Tissue Mechanics Based Method to Improve Tissue Displacement Estimation in Ultrasound Elastography*

Niusha Kheirkhah, Sergio C. H. Dempsey, Hassan Rivaz, Abbas Samani, *Member, IEEE,* and Ali Sadeghi-Naini, *Senior Member, IEEE*

***Abstract*— Cancer is known to induce significant structural changes to tissue. In most cancers, including breast cancer, such changes yield tissue stiffening. As such, imaging tissue stiffness can be used effectively for cancer diagnosis. One such imaging technique, ultrasound elastography, has emerged with the aim of providing a low-cost imaging modality for effective breast cancer diagnosis. In quasi-static breast ultrasound elastography, the breast is stimulated by ultrasound probe, leading to tissue deformation. The tissue displacement data can be estimated using a pair of acquired ultrasound radiofrequency (RF) data pertaining to pre- and post-deformation states. The data can then be used within a mathematical framework to construct an image of the tissue stiffness distribution. Ultrasound RF data is known to include significant noise which lead to corruption of estimated displacement fields, especially the lateral displacements. In this study, we propose a tissue mechanics-based method aiming at improving the quality of estimated displacement data. We applied the method to RF data acquired from a tissue-mimicking phantom. The results indicated that the method is effective in improving the quality of the displacement data.**

***Clinical Relevance*— The developed method can easily be implemented for use with clinical ultrasound systems. The input required here is the tissue displacement field which can be generated using conventional ultrasound motion-tracking methods. The output is an enhanced version of the displacement fields that leads to more reliable elasticity images.**

I. Introduction

Breast cancer is the most diagnosed type of cancer and the second leading cause of cancer death in women. In 2020, it is estimated that more than 270,000 new invasive breast cancer cases will be diagnosed in women while 42,170 women will die from breast cancer in the United States [1]. If diagnosed at early stages, breast cancer can be treated more effectively, leading to higher survival rates. Breast cancer tumor development is associated with considerable interaction with stromal cells and connective tissue. As such, breast cancer alters the tissue biomechanical properties significantly. Therefore, ultrasound elastography, which is a non-invasive imaging modality for tissue mechanical characterization, can potentially be used as a clinically viable diagnostic technique for breast cancer. In this work, the focus is on quasi-static ultrasound elastography where the tissue is externally excited by pressing the ultrasound probe against the tissue. In quasi-static elastography, radiofrequency (RF) data is acquired under pre- and post-compression states, before the tissue displacement in axial and lateral directions can be estimated. Next, strain images can be generated by applying spatial derivatives to the estimated displacement fields. Strain images can be used directly as an approximation to the tissue stiffness distribution. While often capable of detecting abnormalities, strain imaging does not provide reliable estimates of the stiffness as it assumes stress uniformity. To account for the tissue stress non-uniformity, elastography image reconstruction algorithms have been developed [2][3]. In these algorithms, first, an inverse problem is formulated based on the theory of elasticity equations before it is solved directly or indirectly to calculate tissue mechanical parameters (e.g. Young's modulus). The input to such frameworks is measured tissue displacement data. The accuracy of this data has a primary impact on the estimation of tissue mechanical parameters. In ultrasound elastography, this data is contaminated by substantial amount of noise originating from the pre- and post-compression ultrasound RF data. Furthermore, in ultrasound elastography the resolution of lateral displacements is lower than that in axial direction, again impacting the quality of elastography images. Research efforts have been made to improve tissue displacement estimation. To that end, methods have been developed that require modifying the US imaging system significantly. For example methods were developed that involved introducing non-axial oscillations/modulations in their respective imaging point spread functions [4][5]. Another example involved using angular compounding to improve lateral displacements [6]. Other methods were also proposed that do not need modification of the US imaging system and rely primarily on image processing to improve displacement estimation. These methods employ time delay estimation (TDE) methods which follow regularized optimization-based or window-based approaches. An example of a regularized optimization-based method was developed based on analytical minimization (AM)

*This research has been supported by the Natural Sciences and Engineering Research Council of Canada (NSERC).

N. Kheirkhah and S. Dempsey are with the School of Biomedical Engineering, Western University, London, ON, Canada (emails: nkheirkh@uwo.ca and sdempse2@uwo.ca).

H. Rivaz is with the Department of Electrical and Computer Engineering, Concordia University, Montreal, QC, Canada (email: hrivaz@ece.concordia.ca).

A. Samani is with the Departments of Medical Biophysics and Electrical and Computer Engineering, and the School of Biomedical Engineering, Western University, London, ON, Canada. He is also with the Imaging Research Laboratories, Robarts Research Institute, London, ON Canada (e-mail: asamani@uwo.ca).

A. Sadeghi-Naini is with the Department of Electrical Engineering and Computer Science, Lassonde School of Engineering, York University, Toronto, ON, Canada. He is also with the Department of Radiation Oncology and Physical Sciences Platform, Sunnybrook Research Institute, Sunnybrook Health Sciences Centre; and with the Department of Medical Biophysics, University of Toronto, Toronto, ON, Canada (e-mail: asn@yorku.ca).

of cost functions at real-time [7]. In this method, the cost functions incorporate similarity of echo amplitudes and displacement continuity. This technique has drawbacks which result in inaccurate displacement estimation. The inaccuracy can be alleviated by calculating the whole displacement field at once, leading to substantial improvement in displacement estimation [8]. The regularized optimization-based approaches can also be combined with window-based approaches to further improve displacement estimation [9]. In [10], total variation regularization, in addition to displacement smoothing, has been proven useful for obtaining reasonably accurate tissue displacement estimation.

Other methods were developed based on tissue mechanics constraints such as tissue incompressibility to improve the estimation of lateral and axial displacement fields. Other tissue mechanics based methods were also developed which utilize constraints pertaining to displacement field time variations derived from tissue mechanics principles [11]. In [12], tissue incompressibility equation was used to construct lateral displacement based on axial strain measurements. They showed that the constructed lateral displacement field has more accuracy and signal-to-noise ratio (SNR) compared with the one estimated from traditional speckle tracking. In [13], a computational formulation based on coupling the state and adjoint equations is proposed to produce improved displacement fields from their noisy measurements. This method was developed under the assumption of an incompressible linear elastic isotropic material. Furthermore, the displacements showed improvement for a thin sheet under plane stress assumption with known shear modulus of the field. In this study, we propose a method that incorporates a principle of tissue mechanics to increase the accuracy of previously estimated displacement fields. To that end, we first use TDE methods introduced in [7] and [8] to acquire an initial estimate of the displacement fields before refining them using tissue mechanics principle. Unlike [13], the proposed method does not require any estimation of the mechanical properties. We validated this method using a tissue-mimicking phantom study.

II. Methods

A. Improvement of Displacement Field Estimation

Axial and lateral displacement fields can be estimated using two frames of ultrasound RF data acquired at pre- and post-mechanical stimulation of tissue with the US probe. In this study, the method proposed in [7] followed by the global ultrasound elastography (GLUE) method [8] were used to obtain an initial estimation of the axial and lateral displacement fields. The estimated displacement fields had a similar resolution to the RF data. Typical ultrasound RF data consists of 200 to 500 RF-lines, each consisting of 1000 to 2000 samples depending on the sampling frequency. Our proposed technique is initiated by down sampling the displacement fields to avoid excessive computation. This was done by laying a new computation grid on the field of view (FOV) based on the new resolution and fitting a 2D quadratic function to each subset of nodal displacements in the old grid surrounding the nodes in the new grid. This data fitting ensures taking advantage of the data high resolution. The down-sampled resolution was the same in the lateral direction and approximately 10 times lower in the axial direction.

For refining the down-sampled displacement fields, we impose mechanics principle governing tissue deformation after smoothing the field using Laplacian filtering. As such, the proposed method proceeds with the following two steps:

1) Laplacian Filtering

Here, the Laplacian is a 2D isotropic operator involving the second spatial derivatives of a field. It highlights regions of sharp intensity changes. To ensure displacement continuity, smoothing the down-sampled displacement field is performed through minimizing the Laplacian of the field. The Laplacian $L(x,y)$ of a field (U) is given by:

$$L(x,y) = \frac{\partial^2 U}{\partial x^2} + \frac{\partial^2 U}{\partial y^2}. \tag{1}$$

The main purpose of this step is to reduce the sharp changes in previously measured displacement values (U_m). This can be achieved using Tikhonov regularization which leads to the following least squares solution:

$$U_{new} = (I + \lambda^2 L^T L) U_m. \tag{2}$$

In the above, L is the finite difference approximation of the Laplacian operator, and λ is the regularization coefficient which determines the tradeoff between the input displacement data U_m and its smoothing extent. The optimal value of λ was calculated by finding the knee point of the plot of $\|L\|$ versus $e = \|U_{new} - U_m\|$ obtained for variable λ values. At this point, the U_{new} field is smooth while it is still close enough to the U_m field.

2) Incompressibility Equation

If a tissue is incompressible, its volume remains constant under deformation. In this case the tissue displacement filed is governed by:

$$\nabla . \nu = 0. \tag{3}$$

In the Cartesian coordinates system, the above equation can be written as:

$$\frac{\partial u_x}{\partial x} + \frac{\partial u_y}{\partial y} + \frac{\partial u_z}{\partial z} = 0. \tag{4}$$

Assuming a plane-strain situation, in which the out-of-plane strain is zero, this equation can be reduced to:

$$\frac{\partial u_x}{\partial x} + \frac{\partial u_y}{\partial y} = 0. \tag{5}$$

In the above equation, u_x and u_y are the lateral and axial components of the displacement field, respectively. To further refine the displacement field, this equation is combined as a constraint with the displacement fields obtained from the previous step to obtain the following:

$$\begin{bmatrix} N \\ \mathrm{I} \end{bmatrix} \begin{Bmatrix} u_x \\ u_y \end{Bmatrix} = \begin{Bmatrix} 0 \\ u_{xm} \\ u_{ym} \end{Bmatrix} \Rightarrow A\mathrm{U} = \mathrm{b}. \tag{6}$$

In Equation (6), u_{xm} and u_{ym} are the lateral and axial displacement fields obtained from the previous step, *N* is the finite difference approximation operator of the incompressibility equation, and *I* is the identity matrix.

The accuracy of each displacement component depends strongly on the resolution of the ultrasound system in the respective direction while the displacement noise characteristics is different in the axial and lateral directions. As such, the lateral displacement field is less reliable than the axial displacement field. Furthermore, the accuracy of Equation (5) depends on the accuracy of the plain strain model in capturing the mechanics of loaded tissue. In our proposed method, the various degrees of reliability of each set of equations involved in Equation (6) is considered by using different weight factors. Let W be a diagonal matrix in which $w_{i,i}$ determines the importance of the i^{th} set of equations in Equation (6). Equation (6) consists of three different sets of equations: incompressibility equation, lateral displacements and axial displacements. The idea is to assign different weight ($w_{i,i}$) to each of these sets consistent with their degree of reliability. Finding optimal weight factors is problem dependent and requires rigorous mathematical and experimental development which is beyond the scope of this work. In this study, we used an ad-hoc approach to find the weight factors suitable for the presented phantom study. Specifically, we applied the commonly used assumption that the SNR for axial data is 10 times larger than the lateral counterpart. We also used three weight factors for the incompressibility equation. The weight sets are summarized in Table 1. Considering the weight factor, we can then change Equation (6) to:

$$WAU = Wb. \quad (7)$$

As WA is known to be a real and positive definite matrix, Equation (7) can be solved using conjugate gradient methods. Here, the Polak-Ribiere method was used for calculating U. The strain fields can be generated by spatially differentiating the calculated displacement fields using the following:

$$\varepsilon_{xx} = \frac{\partial u_x}{\partial x}; \quad \varepsilon_{yy} = \frac{\partial u_y}{\partial y}; \; \varepsilon_{xy} = \frac{\partial u_x}{\partial y}. \quad (8)$$

In the above equation, ε_{xx} and ε_{yy} are the axial and lateral strains, respectively.

B. Phantom Study Validation

The proposed method was validated using the RF data acquired from a block-shaped tissue-mimicking phantom manufactured by the Computerized Imaging Reference Systems (CIRS; Norfolk, VA). The US probe was controlled with a mechanical device to compress the phantom with 0.1 inch steps. The depth of the phantom is large enough for using a plane-strain approximation.

The method was applied on previously estimated displacement fields using the weight sets given in Table 1. The results were then evaluated quantitatively using the compatibility equation which ensures continuity of the displacement field. The 2-D compatibility equation is:

$$\frac{\partial^2 \varepsilon_{xx}}{\partial y^2} + \frac{\partial^2 \varepsilon_{yy}}{\partial x^2} - 2\frac{\partial^2 \varepsilon_{xy}}{\partial x \partial y} = 0. \quad (9)$$

Using the finite difference form of Equation (9), a compatibility matrix was calculated for the strain sets derived from the refined displacements and used as a criterion for evaluating the method applied with each weight set.

TABLE 1. APPLIED WEIGHT SETS

Weight Set	Weight		
	Incompressibility Equation	*Lateral Displacement*	*Axial Displacement*
WS1	1	1	10
WS2	5	1	10
WS3	10	1	10

III. RESULTS

Fig. 1 shows the axial and lateral displacement and strain fields generated using the GLUE method. The refined displacement and strain fields obtained with the weight sets of Table 1 are illustrated in Fig. 2 and Fig. 3, respectively. Fig. 4 shows the norm of compatibility matrix for each weight set.

IV. CONCLUSION

In this study, a new method was proposed for refining displacement and strain fields estimated from ultrasound RF data. This method is based on mechanics principles of tissue deformation. The method was applied to a set of RF data pertaining to a tissue mimicking phantom. We used three different weight sets while incorporating the incompressibility equation as a constraint. The weight sets chosen for the measured lateral and axial displacement were consistent with the estimated SNR of the displacement fields in different directions. Furthermore, we used three different weight sets for the incompressibility equation which correspond to different levels of reliability of the plain strain model. Comparing the initial strain images shown in the bottom row of Fig. 1 with corresponding images in Fig. 3 clearly shows qualitative improvement as the obtained images are considerably cleaner. For quantitative assessment, we evaluated the results based on the norm of the compatibility matrix criterion. According to Equation (9), ideally this norm should be equal to 0. Fig. 4 shows that, irrespective of the chosen weight set, the proposed method reduced the value of this norm drastically, making the estimated displacement field

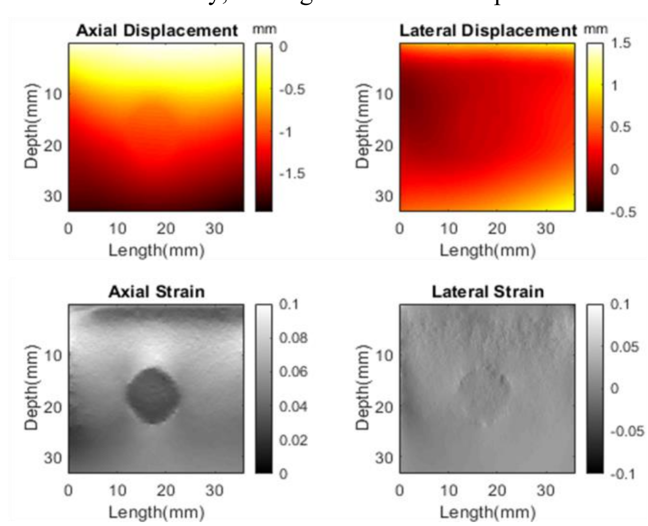

Figure 1. The phantom's displacement and strain fields generated using the GLUE method

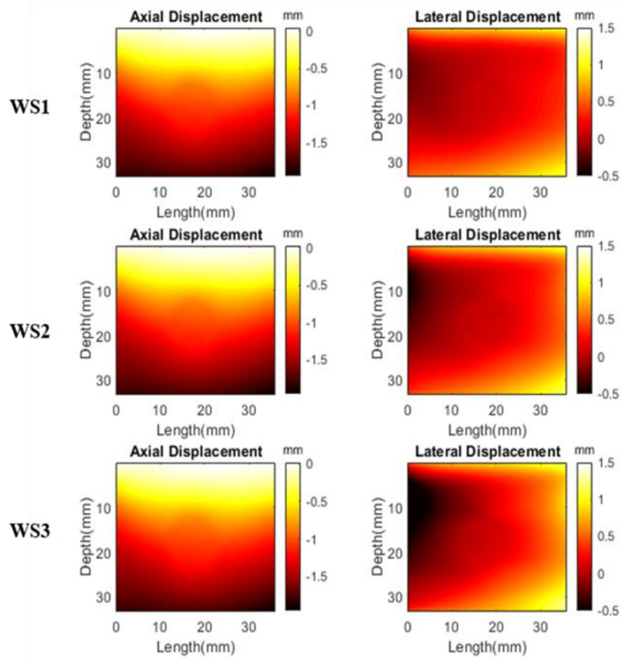

Figure 2. Refined displacement data for different weight sets

close to compatible. The results showed that the proposed method is not very sensitive to the chosen weight set as long as reasonable values are considered. Between the axial and lateral displacements, the level of improvement of the lateral displacement was higher. This is interesting as current US motion estimation methods have a major weakness in capturing the lateral displacements. The depth of the phantom used in this study was large enough for the plane strain model approximation. While not exactly valid because the width of the transducer smaller than the width of the phantom, Equation (5) presents a good approximation, hence the results

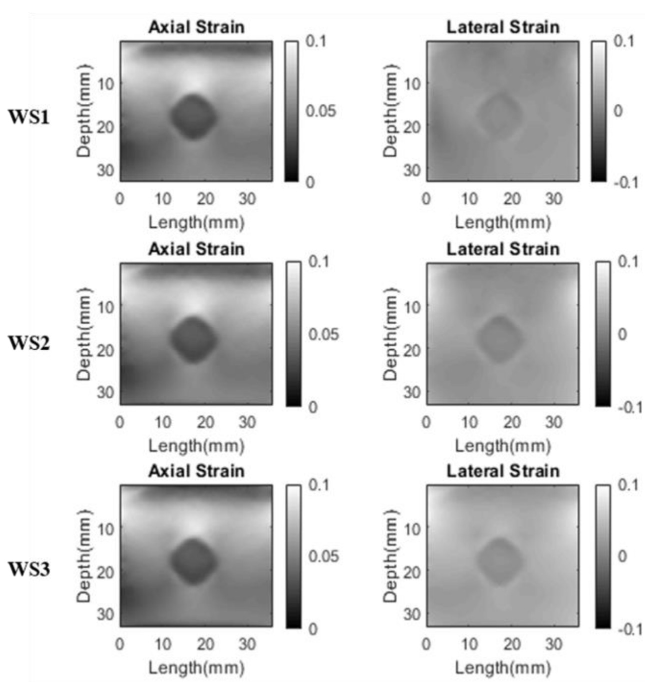

Figure 3. Refined strain data for different weight sets

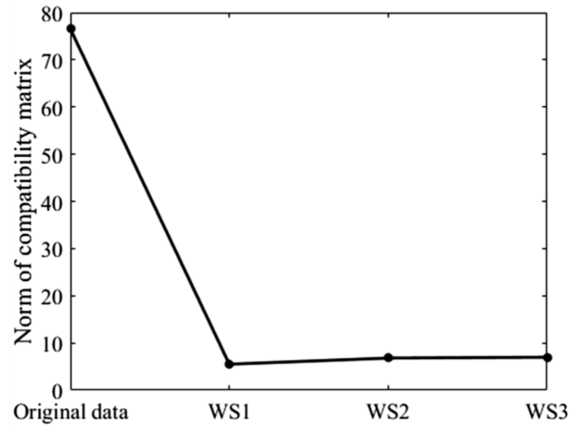

Figure 4. Norm of compatibility matrix calculated for each set of strains

are reliable. It is noteworthy that the accuracy of Equation (5) may not be high with breast clinical data since the plane strain assumption becomes questionable. As such, further model development is required for clinical studies. One viable option for such development is deriving an approximate relationship to the out-of-plane strain using suitable mechanical models before incorporation in Equation (5).

REFERENCES

[1] "American Cancer Society | Information and Resources about for Cancer: Breast, Colon, Lung, Prostate, Skin." [Online]. Available: https://www.cancer.org/. [Accessed: 22-Jan-2020].

[2] A. Samani, J. Bishop, and D. B. Plewes, "A constrained modulus reconstruction technique for breast cancer assessment," *IEEE Trans. Med. Imaging*, vol. 20, no. 9, pp. 877–885, 2001.

[3] M. M. Doyley, P. M. Meaney, and J. C. Bamber, "Evaluation of an iterative reconstruction method for quantitative elastography," *Phys. Med. Biol.*, vol. 45, no. 6, pp. 1521–1540, Jun. 2000.

[4] J. A. Jensen and P. Munk, "A new method for estimation of velocity vectors," *IEEE Trans. Ultrason. Ferroelectr. Freq. Control*, vol. 45, no. 3, pp. 837–851, 1998.

[5] M. E. Andcrson, "Multi-dimensional velocity estimation with ultrasound using spatial quadrature," *IEEE Trans. Ultrason. Ferroelectr. Freq. Control*, vol. 45, no. 3, pp. 852–861, 1998.

[6] U. Techavipoo, Q. Chen, T. Varghese, and J. A. Zagzebski, "Estimation of displacement vectors and strain tensors in elastography using angular insonifications," *IEEE Trans. Med. Imaging*, vol. 23, no. 12, pp. 1479–1489, Dec. 2004.

[7] H. Rivaz, E. M. Boctor, M. A. Choti, and G. D. Hager, "Real-time regularized ultrasound elastography," *IEEE Trans. Med. Imaging*, vol. 30, no. 4, pp. 928–945, 2011.

[8] H. S. Hashemi and H. Rivaz, "Global Time-Delay Estimation in Ultrasound Elastography," *IEEE Trans. Ultrason. Ferroelectr. Freq. Control*, vol. 64, no. 10, pp. 1625–1636, 2017.

[9] M. Ashikuzzaman, C. J. Gauthier, and H. Rivaz, "Global ultrasound elastography in spatial and temporal domains," *IEEE Trans. Ultrason. Ferroelectr. Freq. Control*, vol. 66, no. 5, pp. 876–887, May 2019.

[10] U. Albocher, P. E. Barbone, M. S. Richards, A. A. Oberai, and I. Harari, "Approaches to accommodate noisy data in the direct solution of inverse problems in incompressible plane strain elasticity," *Inverse Probl. Sci. Eng.*, vol. 22, no. 8, pp. 1307–1328, Nov. 2014.

[11] H. Rivaz, E. M. Boctor, M. A. Choti, and G. D. Hager, "Ultrasound elastography using multiple images," *Med. Image Anal.*, vol. 18, no. 2, pp. 314–329, 2014.

[12] M. A. Lubinski, "Lateral displacement estimation using tissue incompressibility," *IEEE Trans. Ultrason. Ferroelectr. Freq. Control*, vol. 43, no. 2, pp. 247–256, 1996.

[13] D. T. Seidl, A. A. Oberai, and P. E. Barbone, "The Coupled Adjoint-State Equation in forward and inverse linear elasticity: Incompressible plane stress," *Comput. Methods Appl. Mech. Eng.*, vol. 357, Dec. 2019.